Optimization of lapping process parameters of CP-Ti based on PSO with mutation and BPNN

Kaiqiang Ye (1239075922@qq.com)
Anhui Polytechnic University https://orcid.org/0000-0002-8351-4466
Jianbin Wang
Anhui Polytechnic University https://orcid.org/0000-0002-2594-3326
Hong Gao
Anhui Polytechnic University
Liu Yang
Anhui Polytechnic University
Ping Xiao
Anhui Polytechnic University

Research Article

Keywords: Particle swarm optimization(PSO), BP neural network(BPNN), Parameter optimization, Commercial pure titanium(CP-Ti), Free abrasive lapping, K-fold cross validation

Posted Date: March 30th, 2021

DOI: https://doi.org/10.21203/rs.3.rs-364458/v1

Version of Record: A version of this preprint was published at The International Journal of Advanced Manufacturing Technology on August 19th, 2021. See the published version at https://doi.org/10.1007/s00170-021-07862-1.

Optimization of lapping process parameters of CP-Ti based on PSO with mutation and BPNN

Kaiqiang Ye [1] · Jianbin Wang [1] · Hong Gao [1] · Liu Yang [1] · Ping Xiao [1, 2]

[1] School of Mechanical Engineering, Anhui Polytechnic University, Wuhu 241000, People's Republic of China

[2] School of Engineering, University of Bridgeport, Bridgeport 06604, the United States of America

✉ Jianbin Wang
wjb@ahpu.edu.cn

Abstract This work aims to improve the surface quality of commercially pure titanium (CP-Ti) with free alumina lapping fluid and establish the relationship between the main process parameters of lapping and roughness. On this basis, the optimal process parameters were searched by performing particle swarm optimization with mutation. First, free alumina lapping fluid was used to perform an $L_9(3^3)$ orthogonal experiment on CP-Ti to acquire data samples to train the neural network. At the same time, a BP neural network was created to fit the nonlinear functional relation among the lapping pressure P, spindle speed n, slurry flow Q and roughness Ra. Then, the range of the node numbers in the hidden layer of the neural network was determined by empirical formulas and the Kolmogorov theorem. On this basis, particle swarm optimization with mutation was used to search for the optimal process parameter configurations for lapping CP-Ti. The optimal process parameter configurations were used in the neural network to calculate the prediction value. Finally, the accuracy of the prediction was verified experimentally. The optimum process parameter configurations found by particle swarm optimization were as follows: the lapping pressure was 5 kPa, spindle speed was 60 r·min^{-1} and slurry flow was 50 ml·min^{-1}. Then, the configurations were applied to a neural network to simulate prediction: the roughness was 0.1127 μm. The roughness obtained by experiments was 0.1134 μm. The error was 0.62%, which indicates that the well-trained neural network can achieve a good prediction when experimental data are missing. Applying the particle swarm optimization (PSO) algorithm with mutation to a neural network will obtain the optimal process parameter configurations, which can effectively improve the surface quality of CP-Ti lapped with free abrasive.

Keywords Particle swarm optimization(PSO); BP neural network(BPNN); Parameter optimization; Commercial pure titanium(CP-Ti); Free abrasive lapping; K-fold cross validation

1 Introduction

Due to its excellent mechanical properties, such as high specific strength and high wear resistance and corrosion resistance, CP-Ti is widely used in aerospace, national defence, chemical and marine fields [1-5]. However, as a typical difficult cutting material, industrially pure titanium cannot be machined well using traditional milling and turning techniques. Therefore, coupled mechanical-chemical lapping has become an important means to achieve the high-efficiency and high-precision machining of CP-Ti and has been deeply studied in recent years. However, how to obtain better surface quality has become a research hot-spot in recent years. Therefore, how to optimize lapping parameters to improve the surface quality of CP-Ti is an important problem.

At present, the methods used to optimize lapping parameters mainly include the quantum-based optimization method [6] /empirical model [7] /optimization algorithm combined with a neural network. The quantum-based optimization method uses the wheel speed, work piece speed, depth of dressing and lead of dressing as control parameters. Minimal production costs, maximal production rates and minimal surface roughness are the optimization criteria being pursued [6]. However, the surface roughness is influenced by many factors in the lapping process; therefore, the quantum-based optimization method is not an effective solution to the problem; as such, it is difficult to quickly and accurately forecast the roughness using the quantum-based optimization method. The empirical model uses the wheel speed, abrasive concentration, current, and pulse on time as control parameters. However, this method simultaneously analyses only two influencing factors for the surface roughness , which means that this method can only analyse the influence of each pair of parameters on the surface roughness. Hence, we need a method that can simultaneously consider all the parameters.

Furthermore, the neural network method could predict the surface roughness based on the limited values measured in the lapping experiment. For this reason, the neural network method has integrated advantages over the quantum-based optimization method/empirical model in terms of the experimental quantities and result reliability [8]. The highly parallel structure of the neural network enables it to complete the parallel implementation process, so it has better fault tolerance and faster overall processing speed than the quantum-based optimization method/empirical model. Neural networks have the theoretical ability of approximatingto approximate arbitrary nonlinear maps. It applies a new method to the nonlinear control problem. A well-trained neural network has the ability to generalize all data. Therefore, neural networks can solve the control process problem, which is difficult to address using mathematical models or descriptive rules. Therefore, the neural network method has been broadly utilized to predict the pulling force [9], surface roughness [10] and lapping capability of power plant ball mills [11].

As a very simple neural network, BP neural networks are widely used in many fields. Huan Zhou et al [12] proposed a GA-BP model to predict the lapping forces produced during the creep-feed deep lapping of titanium matrix composites. Comparative results show that the GA-BP model has good prediction accuracy. Ma, Dongliang et al [13] used the BP neural network to predict the effect of changing certain parameters, such as heat flux, mass flux, pipe diameter and pressure, on the heat transfer coefficient of supercritical water. The results show that the trained BP neural network prediction model can be applied to achieve a better prediction and understanding of the heat transfer coefficient of supercritical water. Liu, Yongkuo et al [14]proposed the continuous and dynamic prediction of the time series of NPP operating parameters. Validation results indicated that the proposed model could be used to achieve a stable prediction effect with high prediction accuracy for the prediction of fluctuating data.

However, the BP neural network can only solve prediction and classification problems and cannot handle parameter optimization problems. Therefore, it needs to be combined with the optimization algorithm. Jidong Wang et al [15] used the improved particle swarm optimization (PSO) algorithm to optimize the previous model. The simulation results of a practical example show that the proposed wind power range prediction model can effectively forecast the output power interval and provide power grid dispatchers with decisions. Qi, Jiangtao et al [16] optimized the influence of normal milk processing and mixing performance by response surface analysis and the BP GA neural network algorithm. The results revealed that the BP-GA neural network algorithm has better fitting performance than response surface analysis and confirmed the optimal working parameter combination that could provide a reference to improve double blade normal milk processing and mixing device design and milk processing quality. Wang, Wei et al [17] developed a method to predict the thermal performance of PTC systems based on a GA-BP neural network model. The results revealed that the GA-BP neural network model can be successfully used to predict the complex nonlinear relationship between the input variables and thermal performance of PTC systems. Zhang, Q [18] designed the PSO-GA-BP model to assess personal credit risk, which makes up for the shortcomings of traditional BP network parameter training and improves the efficiency and accuracy of prediction. Gao, Guanbin et al [19] proposed a novel hybrid algorithm that employs BPNN and PSO algorithms for the kinematic parameter identification of industrial robots with an enhanced convergence response. The results show that the proposed parameter-identification method based on the BPNN and PSO has fewer

iterations and faster convergence speed than the standard PSO algorithm. For the above reasons, in the present work, a BP neural network combined with the PSO algorithm is proposed to optimize the lapping process parameters of CP-Ti. Furthermore, the prediction results are verified by experiments. The optimum lapping parameters are accordingly given.

2 Neural network model

2.1 Test details

In this experiment, square commercially pure titanium samples with side lengths of 25 mm were selected as the processed parts. To ensure that the other parameters were the same before lapping, all samples were pretreated, i.e., #240 sandpaper was used to grind the samples for 3 min. After pretreatment, the average surface roughness (Ra) of the samples was 0.644 μm.

To reduce the number of tests and the cost as much as possible, the $L_9(3^3)$ orthogonal test was used to explore the influence of the main lapping process parameters on the surface roughness of the lapping samples. The process parameters used in the test include lapping pressure, spindle speed and lapping fluid flow. According to the empirical values of each process parameter, the corresponding $L_9(3^3)$ orthogonal test was developed, and the factor level is shown in Table 1.

Tab. 1 Factor level

Level	Lapping pressure p/(kPa)	Spindle speed n/ (r·min^{-1})	Slurry flow Q/ (ml·min^{-1})
1	2.4	40	40
2	4.0	60	60
3	5.6	80	80

As shown in Fig. 1, the lapping pad is fixed on the lapping plate and rotates together with the lapping plate. The CP-Ti sample is sealed on the pressing plate with wax and fixed on the carrier together with the pressing plate. In the lapping process, the lapping liquid is added at a certain flow rate and reacts with the sample surface. Then, the reaction layer on the workpiece surface is removed by mechanical action so that the workpiece surface material can be quickly removed. Under the joint action and promotion of mechanical lapping and chemical lapping, the surface of the workpiece is machined flat.

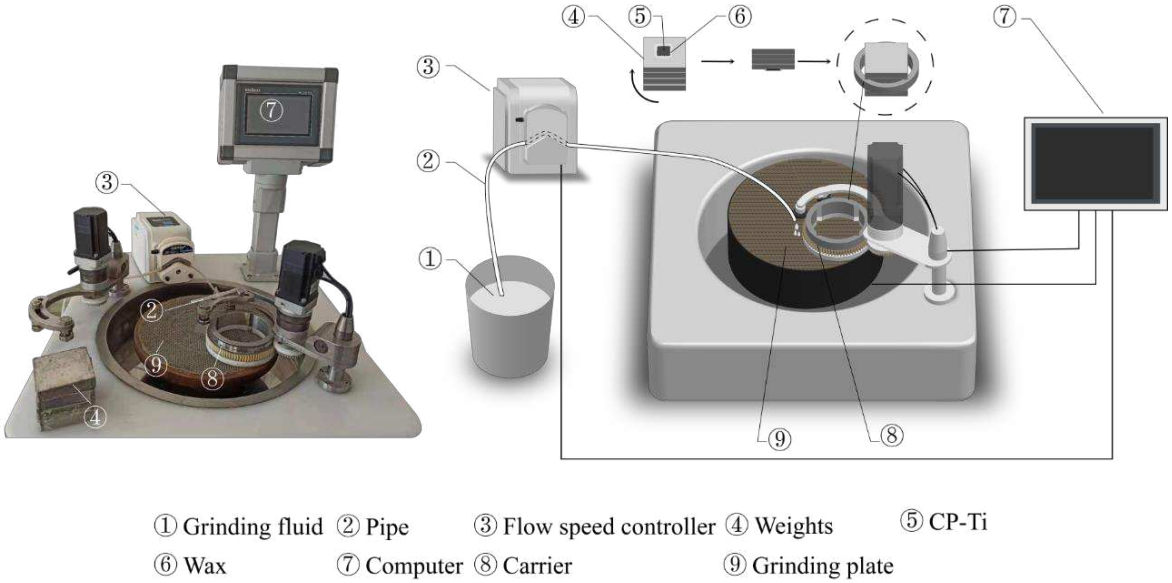

Fig. 1 Schematic diagram of the lapping principle

2.2 Data preprocessing

After the samples were ground, they were cleaned by an ultrasonic cleaning machine for 15 min and blown dried with an electric hair dryer. Then, a 3D surface topography analyser (PS50) was used to randomly pick five points on the sample surface for testing, and the average value of the detected surface roughness was taken as the measured surface roughness. The test results are shown in Table 2.

Tab. 2 Result of the orthogonal test

Experiment number	Lapping pressure p/kPa	Spindle speed n/ (r·min^{-1})	Slurry flow Q / (ml·min^{-1})	Roughness Ra/μm
1	2.4	40	40	0.341
2	2.4	80	60	0.209
3	2.4	60	80	0.470
4	4	60	40	0.177
5	4	40	60	0.265
6	4	80	80	0.316
7	5.6	80	40	0.171
8	5.6	60	60	0.116
9	5.6	40	80	0.510

To remove the effects of dimensional differences and avoid situations where small data are overwhelmed by big data, the input and output data need to be normalized. Formula (1) is used to normalize input data

$$x_{nor} = 2\frac{x - x_{\min}}{x_{\max} - x_{\min}} - 1 \tag{1}$$

where $x_{nor} \in [-1,1]$ is the normalized input data; x is the input data to be normalized; x_{min} is the minimum value in this type of data; and x_{max} is the maximum value in this type of data.

To extend the coverage of the output data, formula (1) is not used to directly normalize the output data. Instead, a broader value range is defined to normalize the output data, as shown in Formula (2) :

$$y_{nor} = 2\frac{y - y'_{\min}}{y'_{\max} - y'_{\min}} - 1 \tag{2}$$

where $y_{nor} \in [-1,1]$ is the normalized output data; y is the normalized output data; $y'_{\min}$ is 0.08; and $y'_{\max}$ is 0.6.

2.3 Neural network architecture

Because the data obtained from orthogonal experiments are limited, it is difficult to train a complex network model. Therefore, the most compact three-layer neural network is selected. Since the dimensions of the input and output data are 3 and 1, respectively, the neuron nodes of the input and output layers are set to 3 and 1, respectively. The number of neuron nodes in the hidden layer can be derived from empirical formula (3) and Kolmogorov's theorem.

$$m_1 = \sqrt{u + v} + a \tag{3}$$

where m_1 is the range of the number of nodes in the hidden layer derived from empirical formula (3). Decimals are rounded up. a usually takes an integer from 1 to 10, so the range of m_1 values is 3 to 12.

According to Kolmogorov's theorem, any n-element continuous function can be represented by the sum of a cluster of continuous functions, and the number of functions is not more than 2n+1. Therefore, the value range of the number of neuron nodes in the hidden layer is also computed by empirical formula (4):

$$m_2 \le 2u+1 \tag{4}$$

where m_2 is the empirical value of the number of nodes in the hidden layer calculated by Kolmogorov theorem, and its value ranges from 1 to 7.

Combined with the value range of m_1 and m_2, it can be concluded that the number of neuron nodes in the hidden layer ranges from 3 to 7. The optimal number of neuron nodes in the hidden layer will be obtained by comparing the prediction accuracy before and after training.

In addition, the final network architecture was completed after the activation function, loss function and optimization algorithm were selected. On the one hand, the hidden layer activation function is an S-type tangent function *tansig*, which can process the data non-linearly and enable the model to fit the nonlinear function, and the expression is

$$\text{tansig}(x) = 2/(1+\exp(2x)) - 1 \tag{5}$$

On the other hand, the hidden layer activation function is a pure linear function and expressed as

$$purelin(x) = \begin{cases} x & x \ge 0 \\ 0 & x < 0 \end{cases} \tag{6}$$

The loss function is the MSE function and is expressed as

$$loss = \sum_{j=1}^{n} (y_{pred}^{j} - y_{real}^{j})^2 \Big/ n \tag{7}$$

where *loss* is the loss value calculated by MSE, y_{pred}^{j} is the predicted output given after the *j*th sample y_{real}^{j} is substituted into the neural network, y_{real}^{j} is the true value of the *j*th sample, and *n* is the total number of samples. The larger the *loss* is, the more the prediction result of the model deviates from the actual situation. The smaller the *loss* is, the closer the prediction result of the model is to the actual situation.

The Levenberg-Marquardt algorithm is selected as the optimization algorithm and is suitable for small and medium-sized networks with fast convergence speed.

In addition, we introduced k-fold cross validation to the training process to fully exploit each set of data in the absence of data samples. K-fold cross validation randomly divides the data into k groups and then takes each subset as a validation set and the remaining k-1 groups as a training set, which will train the neural network in turn to ensure that each subset participates in training the neural network.

In summary, the neural network architecture with dimensions of 3×5×1 is shown in Figure 1; the hidden layer activation function is the tansig function, and the output layer uses the pure linear function.

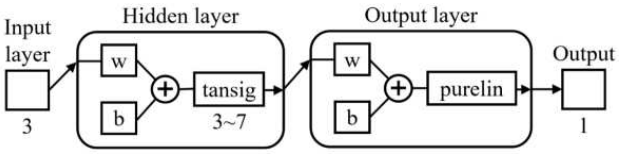

Fig. 2 Architecture diagram of the neural network

3 Variant particle swarm optimization algorithm

PSO was first proposed by Kennedy and Eberbart by observing the predation behaviour of birds. The easiest and most efficient way for birds to find food is to search an area near which food has been found. The optimization algorithm aims to minimize the surface roughness of the work-piece. The lapping pressure, spindle speed and lapping fluid flow were taken as the design variables. Then, the predicted values were calculated through the BPNN. Finally, the PSO algorithm with mutation was used to search for the optimal process parameter combination. The final model is as follows: the design variable X= [p, n, Q]; the target value $Y=Ra_{min}$; and the constraints are $2.4 \le p \le 5.6$, $40 \le n \le 80$, and $40 \le Q \le 80$, where p, n and Q represent the lapping pressure, spindle speed and lapping fluid flow, respectively.

The initial population setting will increase the computational burden and take extra time for optimization if the number of individuals is set to a higher value, and it may not be able to jump out of the local optimal value if the number of individuals is set to a low value. The value range of the lapping process parameters is shown in Table 4. The model will generate 20 individuals and assign values randomly within the constraints as the initial state of the population.

Tab. 4 Range of lapping process parameters

Process parameters	Lapping pressure p/kPa	Spindle speed n/ ($r \cdot min^{-1}$)	Slurry flow Q / ($ml \cdot min^{-1}$)
Range	2.4-5.6	40-80	40-80

The flow chart of extremum optimization based on the PSO algorithm is shown in Figure 3. At the start of the optimization process, all the particle position information is normalized and substituted into the neural network, which would conclude the fitness value of each particle. Then, the model will save the particle position and velocity information of the highest fitness value of the individual and the group (the lowest surface roughness), which would be used to update the particle position and speed information. By this method, the model continuously searches for new individual extrema

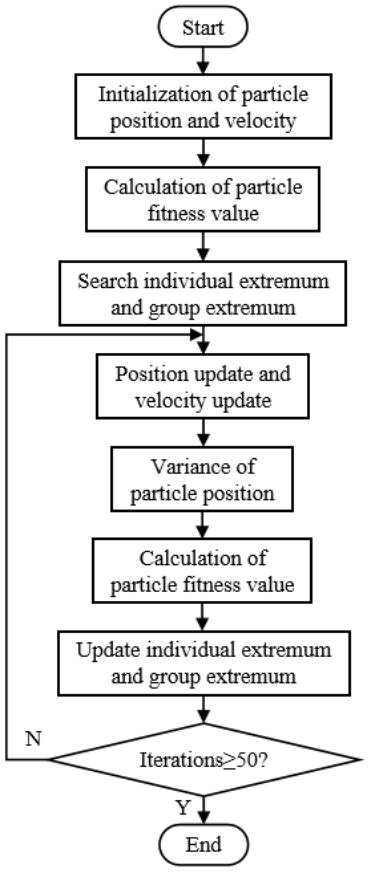

Fig. 3 Flow chart of the optimization of the particle swarm optimization algorithm with mutation

and population extrema and updates the position and velocity information of the remaining particles until the set number of iterations is reached. The position information of a small number of particles is randomized within a given value range to prevent the model from falling into a local optimum after the particle position information is updated.

4 Results and Discussion

4.1 Training and testing the neural network

To more clearly compare the effects of each neural network, the indirect neural network prediction accuracy parameter is adopted and expressed as follows:

$$Accuracy = \exp(-loss) \tag{8}$$

where *loss* is the loss value calculated by MSE, loss∈[0,+∞), and accuracy∈(0,1). The larger the *accuracy* is, the closer the predicted result is to the true value.

After the number of nodes in the hidden layer is set from 3 to 7, the nine sets of data obtained through orthogonal experiments are preprocessed and substituted into the network models with different hidden layer nodes. The training set accuracy after training is shown in Tab. 3. It can be concluded from Tab. 3 that the actual prediction accuracy of the model is the best when the number of neural network nodes is 5. Therefore, the neural network with five nodes is finally selected as the prediction model, and the prediction result is compared with the real value, as shown in Figure 2.

Tab. 3 Neural network prediction accuracy using different numbers of hidden layer nodes

Nodes	3	4	5	6	7
Acc	73.45%	68.98%	83.72%	81.54%	73.30%

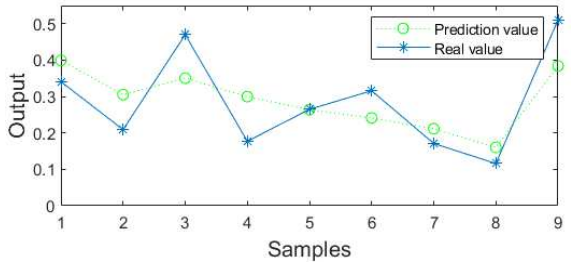

Fig. 2 Prediction comparison with the optimal number of nodes in the hidden layer

4.2 Optimization process

The optimization process of the optimization algorithm is shown in Fig. 4. After 50 iterations, the model obtains the optimal lapping process parameters. The minimum surface roughness value is Y=0.1127; the corresponding optimal lapping process parameter combination is X= [5.1333, 59.3234, 48.7533]. After rounding, the optimal process parameters were a lapping pressure of 4.8 kPa, spindle speed of 60 r·min-1, and lapping fluid flow rate of 50 ml·min^{-1}.

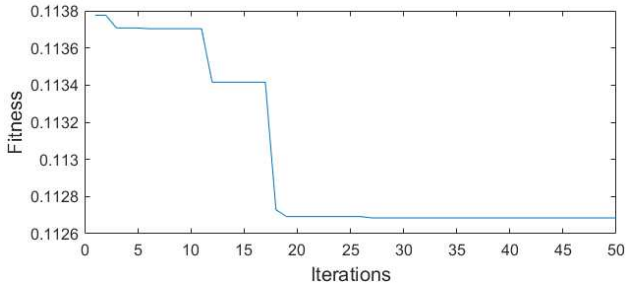

Fig. 4 Fitness diagram

4.3 Verification

When all else is equal, the best lapping process parameters after rounding were chosen to grind CP-Ti samples. After lapping, the samples were measured by a 3D surface topography analyzer (PS50). Five points were randomly selected on the sample surface for testing, and the average value was taken as the measured surface roughness, as shown in Tab. 4.

Tab. 4 Surface roughness

Number	1	2	3	4	5
Ra(μm)	0.102	0.102	0.125	0.123	0.115

The average value of surface roughness $\overline{Ra}$ is as follows:

$$\overline{Ra} = \left(Ra_1 + Ra_2 + Ra_3 + Ra_4 + Ra_5\right)/5 = 0.1134 \tag{9}$$

where $\overline{Ra_i}$ is the *i*th measurement value.

The surface roughness error, the difference between the theoretical value and the measured value, is as follows:

$$Error = \left(Ra_t - Ra_m\right)/Ra_m \approx 0.62\% \tag{10}$$

where Ra_m is the measured surface roughness value and Ra_t is the theoretical surface roughness value.

5 Conclusion

1) A BPNN model was constructed by combining the process parameters for the free abrasive lapping of CP-Ti and the surface roughness of the sample after lapping, and the BPNN model was trained through the data obtained from the orthogonal experiment. Then, the predicted results of the model were evaluated by evaluation index *accuracy*. By comparison, when the number of hidden layer nodes is equal to 5, the prediction accuracy of the model is the highest at 83.72%.

2) After the optimization of the PSO algorithm with mutation, the rounded process parameters were determined. When the lapping pressure was 5 kPa, the spindle speed was 60 r·min^{-1} and the lapping fluid flow was 50 ml·min^{-1}, the surface roughness of the CP-Ti samples was the lowest at 0.1127 μm.

3) The surface roughness measured after lapping was 0.1134 μm, and the surface roughness error predicted by the neural network was within 0.62%, which effectively reduced the surface roughness of CP-Ti and improved the surface quality of CP-Ti.

Declarations

-Ethical Approval('Not applicable')

-Consent to Participate('Not applicable')

-Consent to Publish

The Author confirms:

- that the work described has not been published before (except in the form of an abstract or as part of a published lecture, review, or thesis);
- that it is not under consideration for publication elsewhere;
- that its publication has been approved by all co-authors, if any;
- that its publication has been approved (tacitly or explicitly) by the responsible authorities at the institution where the work is carried out.

The Author agrees to publication in the Journal indicated below and also to
publication of the article in English by Springer in Springer's corresponding English-language journal.
The copyright to the English-language article is transferred to Springer effective if and when the article is accepted for publication. The author warrants that his/her contribution is original and that he/she has full power to make this grant.
The author signs for and accepts responsibility for releasing this material on behalf of any and all co-authors.
The copyright transfer covers the exclusive right to reproduce and distribute the article, including reprints, translations, photographic reproductions, microform, electronic form(offline, online) or any other reproductions of similar nature.

-Authors Contributions

Guarantor of integrity of entire study: Jianbin Wang; Hong Gao

Study concepts: Jianbin Wang; Kaiqiang Ye

Study design: Kaiqiang Ye; Liu Yang

Literature research: Kaiqiang Ye

Experimental studies: Liu Yang; Kaiqiang Ye

Data acquisition: Liu Yang; Jianbin Wang

Data analysis/interpretation: Kaiqiang Ye

Statistical analysis: Kaiqiang Ye

Manuscript preparation: Kaiqiang Ye

Manuscript defnition of intellectual content: Kaiqiang Ye; Ping Xiao

Manuscript editing: Hong Gao; Kaiqiang Ye

Manuscript revision/review: Jianbin Wang; Hong Gao; Kaiqiang Ye

Manuscript fnal version approval: Jianbin Wang

-Funding

The author(s) received the financial support of the Collaborative Innovation Project of Anhui Provincial University (Grant No. GXXT-2019-021), the Key Program in the Excellent Young Talents Support Plan in Universities of Anhui Province (Grant No. gxyqZD2019051), the Young and Middle-aged Talent Training Program of 2018 of Anhui Polytechnic University, the Science and Technology Planning Project of Wuhu City(2020yf20) and Open Research Project of Anhui Simulation Design and Modern Manufacture Engineering Technology Research Center (HuangShan University) (Grant NO. SGCZXYB1804) for the research, authorship, and/or publication of this article.

-Competing Interests

The author(s) declared no potential conflicts of interest with respect to the research, authorship, and/or publication of this article.

-Availability of data and materials

The datasets used or analyzed during the current study are available from the corresponding author on reasonable request.

Reference

1. Ye Y, Kurechu SZ, Sun Z, Matsubara T, Tang G, Hihara T, Okido M, Yashiro H (2018) Self-lubricated nanoporous TiO2-TiN films fabricated on nanocrystalline layer of titanium with enhanced tribological properties. Surf Coat Tech 351:162-170
2. Hamada S, Noguchi H (2020): Fatigue characteristics of a notched specimen made of commercially-pure titanium. Theor Appl Fract Mec 109:1-6
3. Kikuchi S, Ueno A, Akebono H (2020): Combined effects of low temperature nitriding and cold rolling on fatigue properties of commercially pure titanium. Int J Fatigue 139:1-9
4. Chen WQ, Zhang SM, Qiu J (2020): Surface analysis and corrosion behavior of pure titanium under fluoride exposure. J Prosthet Dent 124(2):239
5. Bathini U, Srivatsan TS, Patnaik AK, Menzemer CC (2011): Mechanisms Governing Fatigue, Damage, and Fracture of Commercially Pure Titanium for Viable Aerospace Applications. J Aerospace Eng 24(4):415-424
6. Alajmi MS, Alfares FS, Alfares MS (2019): Selection of optimal conditions in the surface grinding process using the quantum based optimisation method. J Intell Manuf 30(3):1469-1481
7. Ununе DR, Mali HS (2017): Parametric modeling and optimization for abrasive mixed surface electro discharge diamond grinding of Inconel 718 using response surface methodology. Int J Adv Manuf Tech 93(9-12):3859-3872

8. Liu C, Ding W, Li Z, Yang C (2017),: Prediction of high-speed grinding temperature of titanium matrix composites using BP neural network based on PSO algorithm.. Int J Adv Manuf Tech Tech 89(5-8):2277-2285
9. Jain R, Meena ML, Sain MK, Dangayach GS (2019): Pulling force prediction using neural networks. Int J Occup Saf Ergon 25(2):194-199
10. Chandrasekaran M, Devarasiddappa D (2014): Artificial neural network modeling for surface roughness prediction in cylindrical grinding of Al-SiCp metal matrix composites and ANOVA analysis. Adv Prod Eng Manag 9(2):59-70
11. Jiang R, Wang Y, Yan X (2017): Density clustering analysis of fuzzy neural network initialization for grinding capability prediction of power plant ball mill. Multimed Tools Appl 76(17):18137-18151
12. Zhou H, Ding WF, Li Z, Su H-H (2019): Predicting the grinding force of titanium matrix composites using the genetic algorithm optimizing back-propagation neural network model. P I Mech Eng B-J Eng 233(4):1157-1167
13. Ma D, Zhou T, Chen J, Qi S, Alishahzad M, Xiao Z (2017): Supercritical water heat transfer coefficient prediction analysis based on BP neural network. Nucl Eng Des 320:400-408
14. Liu YK, Xie F, Xie CL, Peng MJ, Wu GH, Xia H (2015): Prediction of time series of NPP operating parameters using dynamic model based on BP neural network. Ann Nucl Energy 85:566-575
15. Wang J, Fang K, Pang W, Sun J (2017): Wind Power Interval Prediction Based on Improved PSO and BP Neural Network. J Electr Eng Technol 12(3):989-995
16. Qi J, Zhao W, Kan Z, Meng H, Li Y (2019): Parameter optimization of double-blade normal milk processing and mixing performance based on RSM and BP-GA. Food Sci Nutr 7(11):3501-3512
17. Wang W, Li M, Hassanien HE, Ji ME, Feng Z (2017): Optimization of thermal performance of the parabolic trough solar collector systems based on GA-BP neural network model. Int J Green Energy 14(10):819-830
18. Zhang Q (2017) Personal credit risk assessment of bp neural network commercial banks based on PSO-GA algorithm optimization. Agro Food Ind Hi Tec 28(1):2580-2584
19. Gao G, Liu F, San H, Wu X, Wang W (2018): Hybrid Optimal Kinematic Parameter Identification for an Industrial Robot Based on BPNN-PSO. Complexity 2018:1-11

Figures

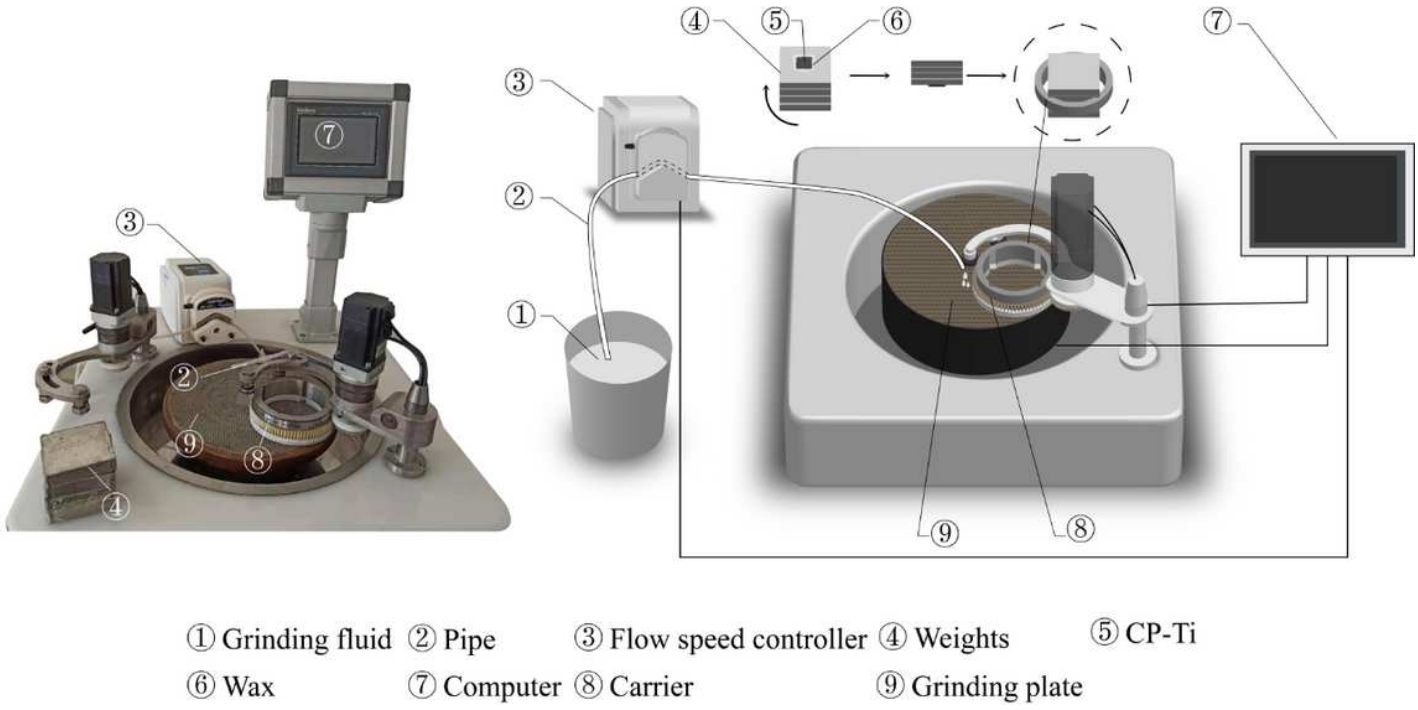

Figure 1

Schematic diagram of the lapping principle

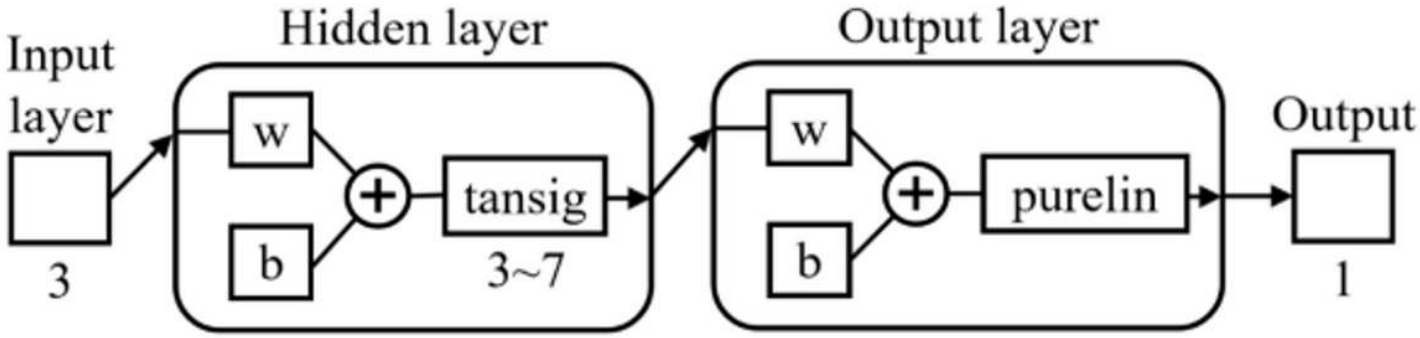

Figure 2

Architecture diagram of the neural network

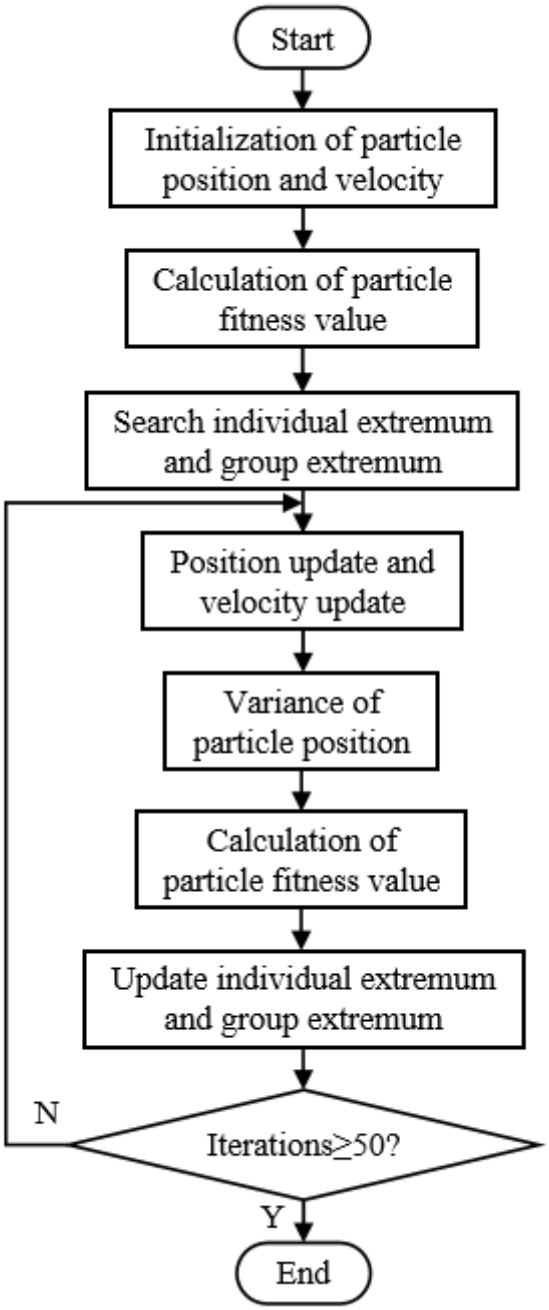

Figure 3

Flow chart of the optimization of the particle swarm optimization algorithm with mutation

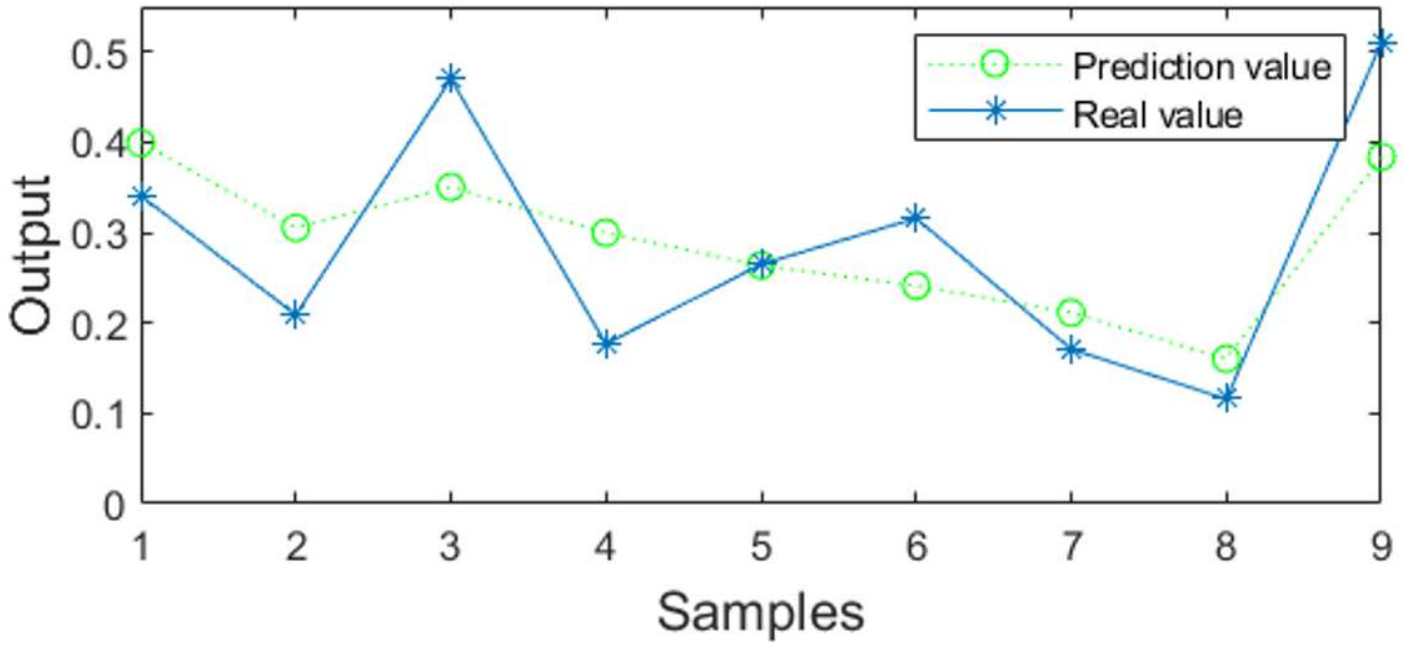

Figure 4

Prediction comparison with the optimal number of nodes in the hidden layer

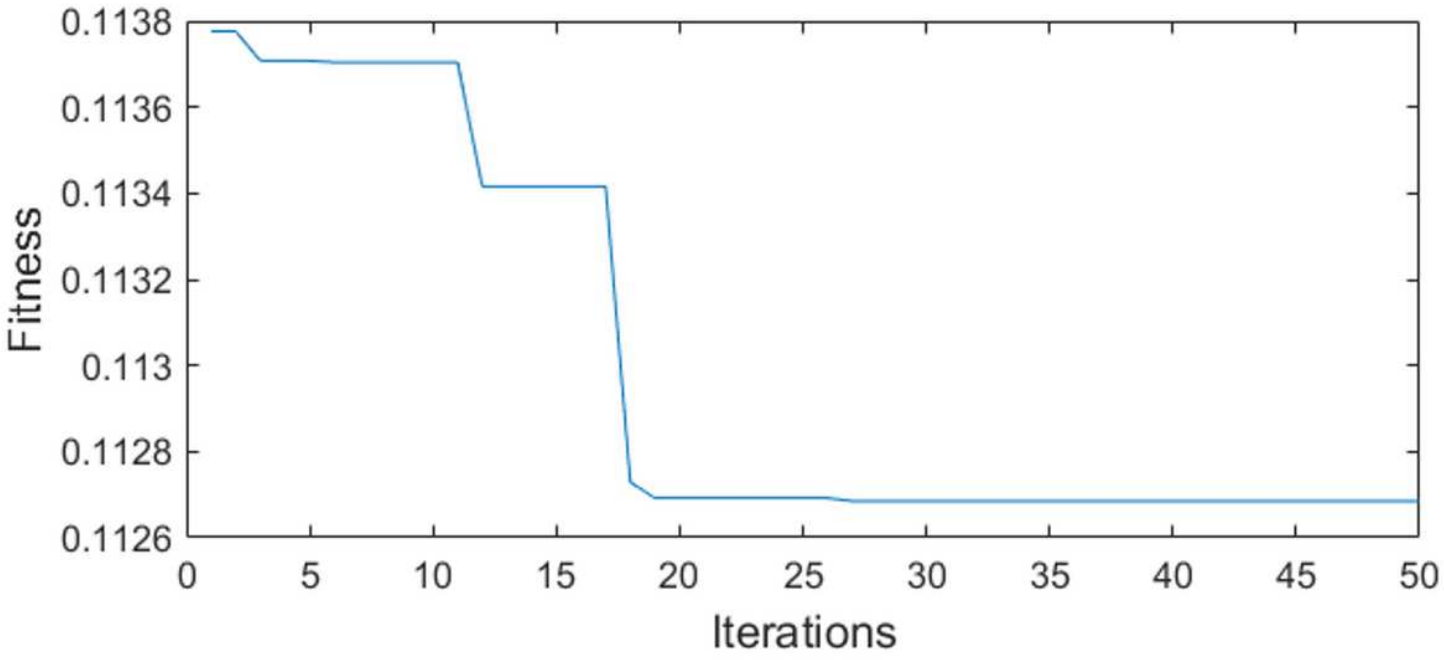

Figure 5

Fitness diagram

Supplementary Files

This is a list of supplementary files associated with this preprint. Click to download.

- MATLABCODE.rtf
- Ra1.tif
- Ra2.tif
- Ra3.tif
- Ra4.tif
- Ra5.tif